Supporting Information

for the article

Relative stability of M/NHC Complexes (M = Ni, Pd, Pt) against R−NHC, X−NHC and X−X couplings in M(0)/M(II) and M(II)/M(IV) catalytic cycles: a theoretical study

Alexander V. Astakhov,[a,b] *Safarmurod B. Soliev,*[a] *Evgeniy G. Gordeev,*[b] *Victor M. Chernyshev*[a,b]
and Valentine P. Ananikov[a,b,*]

[a] Platov South-Russian State Polytechnic University (NPI), Prosveschenya 132, Novocherkassk, 346428, Russia
[b] Zelinsky Institute of Organic Chemistry, Russian Academy of Sciences, Leninsky Prospect 47, Moscow, 119991, Russia

Content

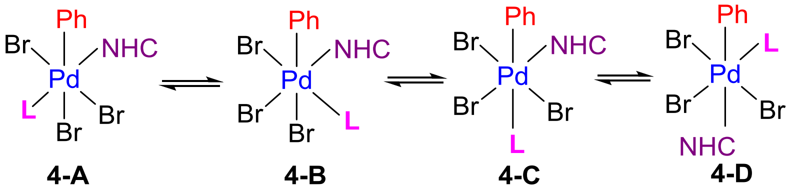

	4-A	4-B	4-C	4-D
ΔG, L = Py	0	15.2	2.0	12.3
ΔG, L = NHC	0	14.1	6.9	——

Scheme S1. Calculated Relative Stabilities (ΔG^{298}, kcal mol^{-1}) of stereoisomers **A-D** of complexes **4-Pd**. NHC = 1,3-dimethylimidazol-2-ylidene.

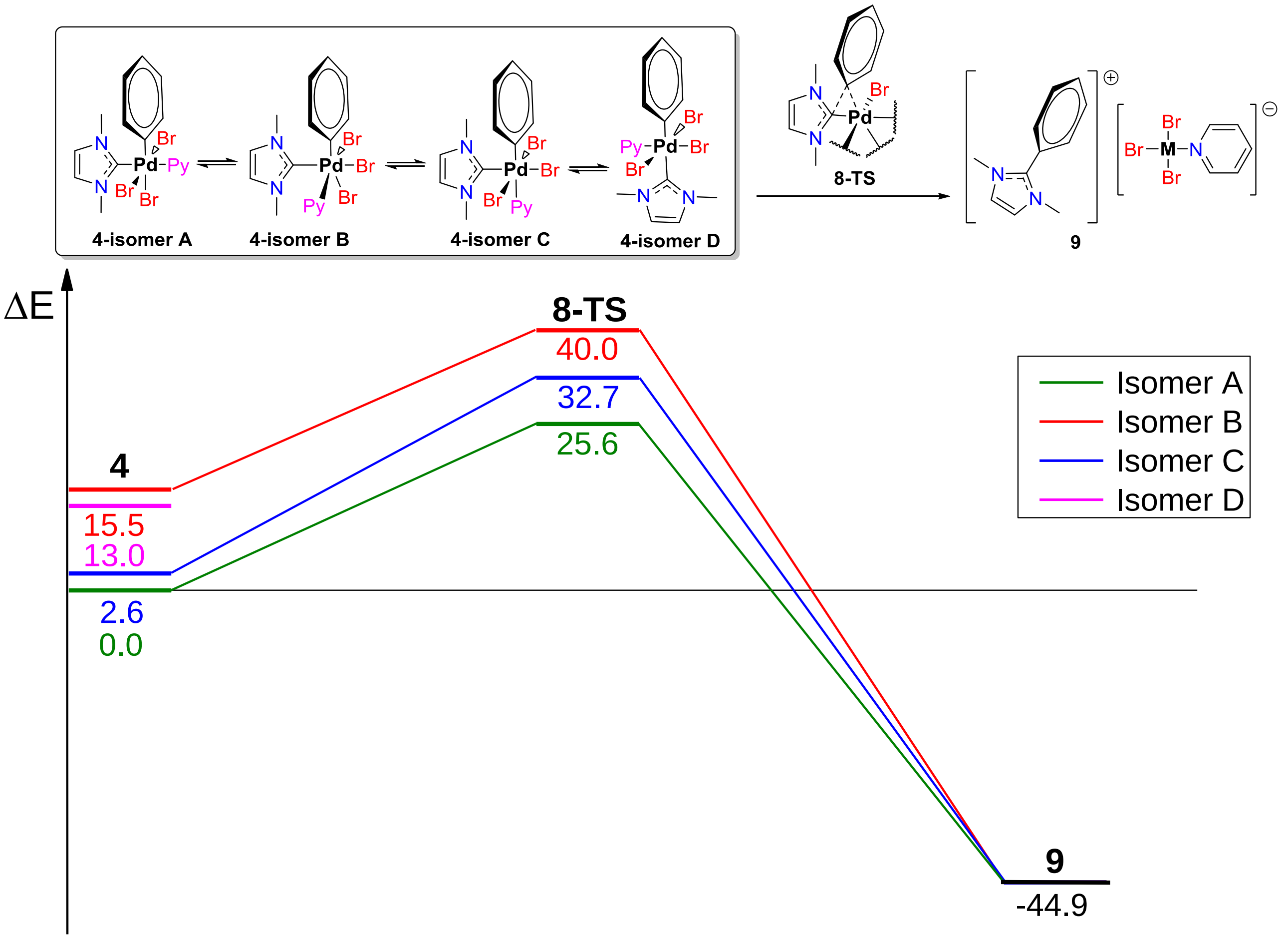

Figure S1. ΔE energy profiles (kcal mol^{-1}) for the Ph−NHC coupling of stereoisomers **A-D** of complexes **4-Pd-Py** calculated at the PBE1PBE/6-311+G(d)&SDD level. NHC = 1,3-dimethylimidazol-2-ylidene. The isomer **D** isomerizes into the isomer **C** or isomer **A** in the course of the reaction (indicated by downward arrows).

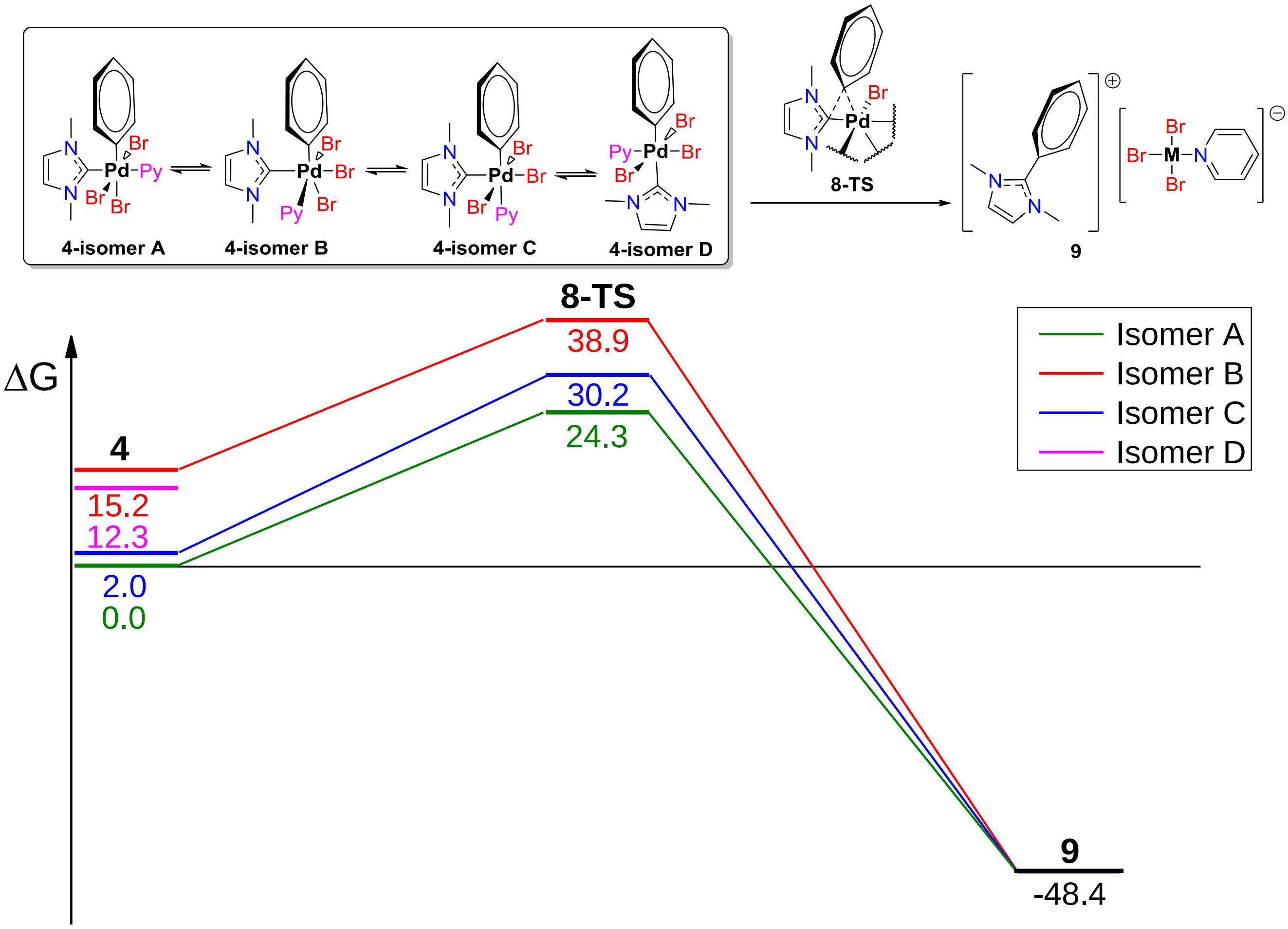

Figure S2. ΔG energy profiles (kcal mol^{-1}) for the Ph−NHC coupling of stereoisomers **A**-**D** of complexes **4-Pd-Py** calculated at the PBE1PBE/6-311+G(d)&SDD level. NHC = 1,3-dimethylimidazol-2-ylidene. The isomer **D** isomerizes into the isomer **C** or isomer **A** in the course of the reaction (indicated by downward arrows).

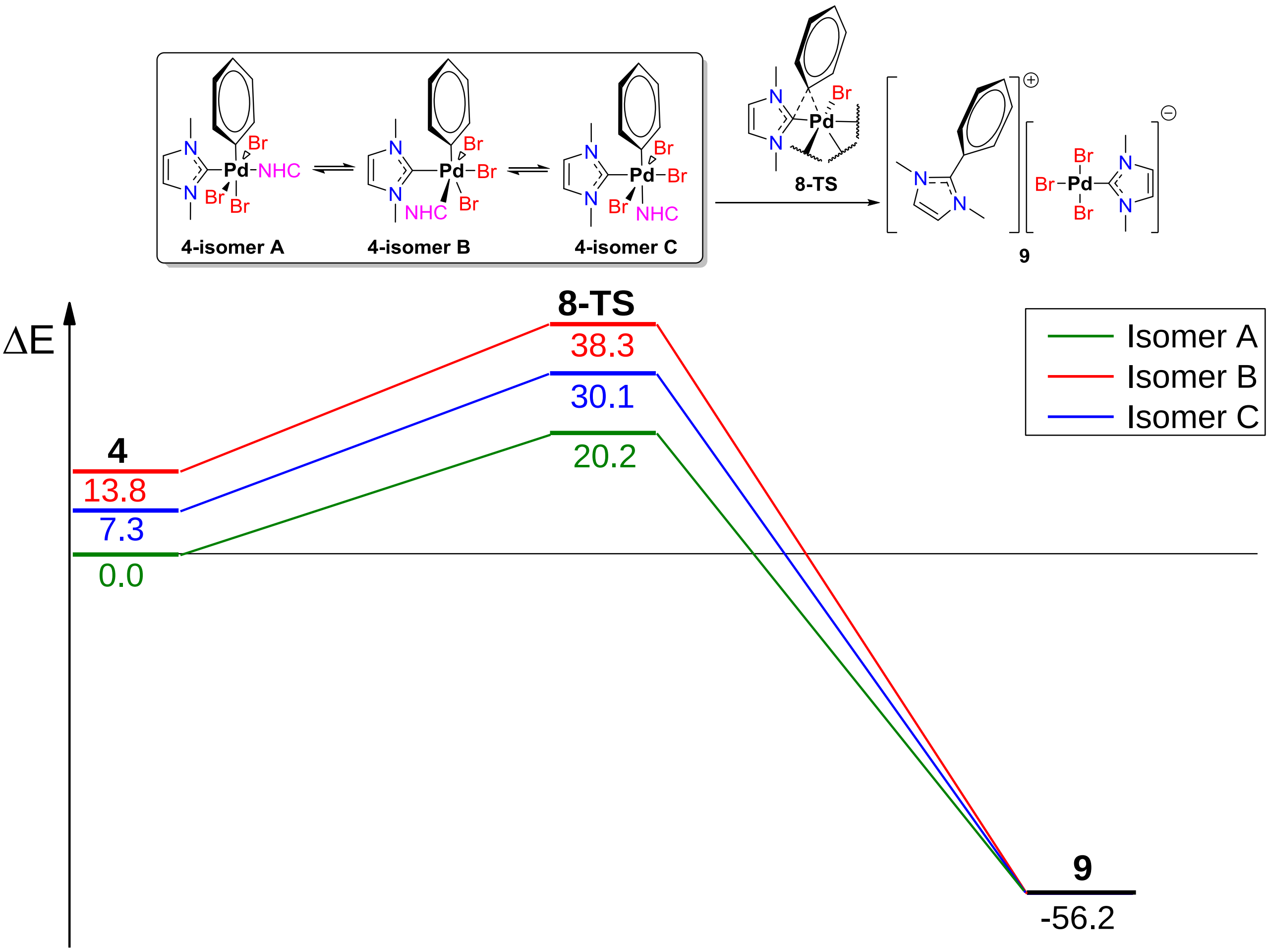

Figure S3. ΔE energy profiles (kcal mol^{-1}) for the Ph–NHC coupling of stereoisomers **A-C** of complexes **4-Pd-NHC** calculated at the PBE1PBE/6-311+G(d)&SDD level. NHC = 1,3-dimethylimidazol-2-ylidene.

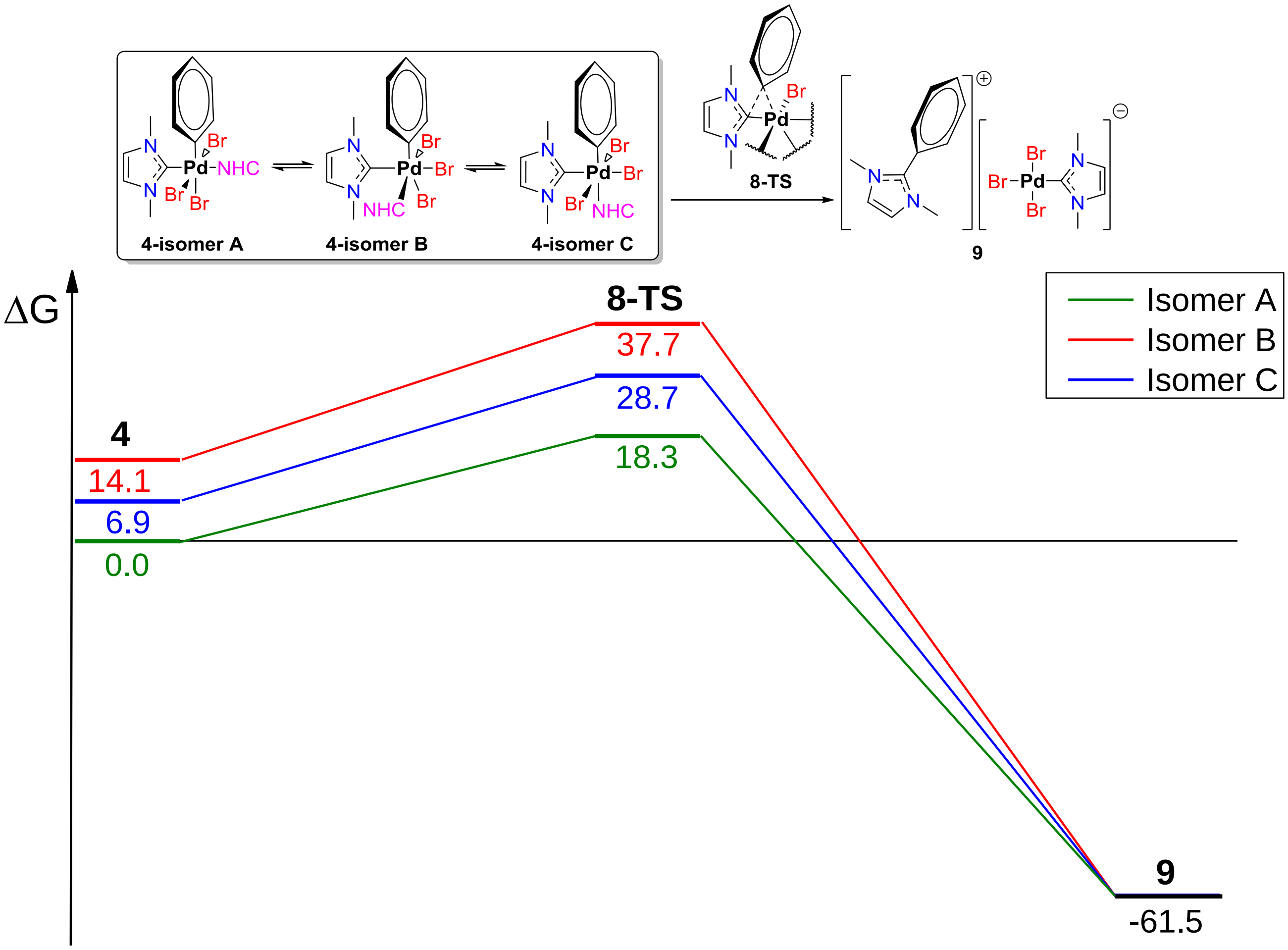

Figure S4. ΔG energy profiles (kcal mol^{-1}) for the Ph−NHC coupling of stereoisomers **A-C** of complexes **4-Pd-NHC** calculated at the PBE1PBE/6-311+G(d)&SDD level. NHC = 1,3-dimethylimidazol-2-ylidene.

Structures for L=Py

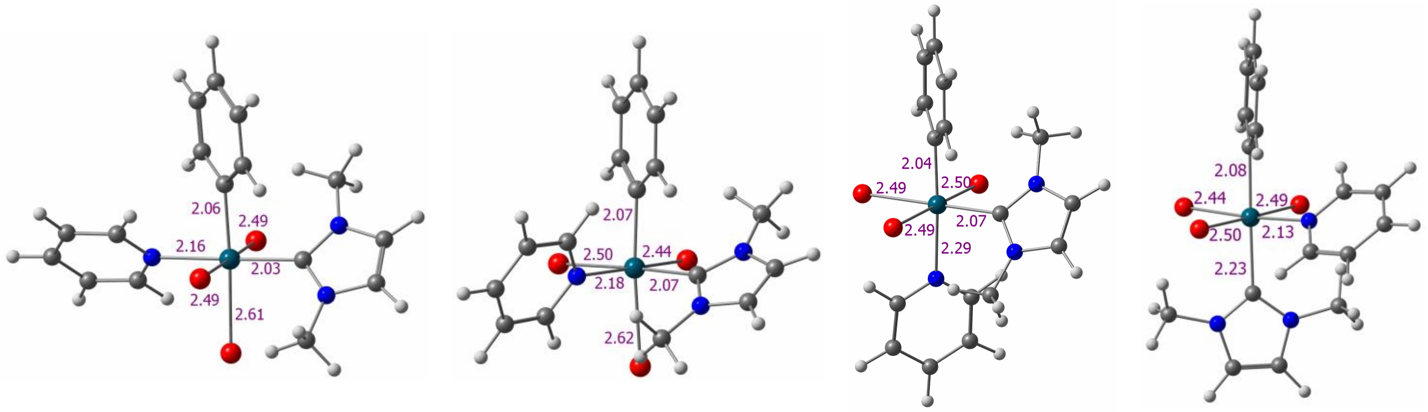

4-A **4-B** **4-C** **4-D**

Structures for L=NHC

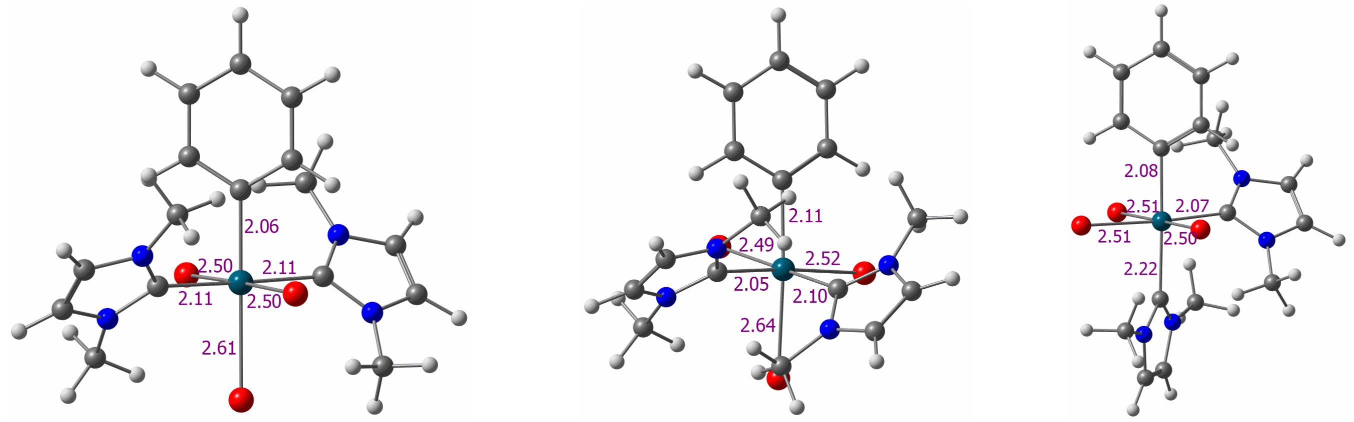

4-A **4-B** **4-C**

Figure S5. Optimized geometries for different stereoisomers of complexes **4** calculated at the PBE1PBE/6-311+G(d)&SDD level. Selected bond distances (Å) are shown in purple.

Table S1. Activation total energies ($\Delta E^{\neq}$), activation enthalpies ($\Delta H^{\neq}$), reaction energies (ΔE) and reaction enthalpies (ΔH) for the R−NHC coupling of complexes **1** (M =Ni, Pd, Pt) at 298 K[a]

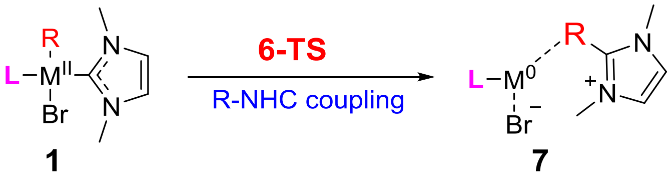

rel. energy, kcal·mol^{-1}	M = Ni	M = Pd	M = Pt
R=Me, L = Py			
$\Delta E^{\neq}_{\mathbf{1\rightarrow 6\text{-}TS}}$	24.7	26.5	46.2
$\Delta E_{\mathbf{1\rightarrow 7}}$	30.3	13.9	32.4
$\Delta H^{\neq}_{\mathbf{1\rightarrow 6\text{-}TS}}$	23.4	25.2	44.3
$\Delta H_{\mathbf{1\rightarrow 7}}$	31.2	14.3	32.9
R=Ph, L = Py			
$\Delta E^{\neq}_{\mathbf{1\rightarrow 6\text{-}TS}}$	22.9	24.7	44.9
$\Delta E_{\mathbf{1\rightarrow 7}}$	13.6	12.5	33.9
$\Delta H^{\neq}_{\mathbf{1\rightarrow 6\text{-}TS}}$	21.5	23.4	43.3
$\Delta H_{\mathbf{1\rightarrow 7}}$	13.8	12.7	33.9
R=Vinyl, L = Py			
$\Delta E^{\neq}_{\mathbf{1\rightarrow 6\text{-}TS}}$	20.6	20.8	40.6
$\Delta E_{\mathbf{1\rightarrow 7}}$	-14.4	-12.5	3.9
$\Delta H^{\neq}_{\mathbf{1\rightarrow 6\text{-}TS}}$	19.3	19.5	39.0
$\Delta H_{\mathbf{1\rightarrow 7}}$	-13.5	-11.6	4.7
R=Ethynyl, L = Py			
$\Delta E^{\neq}_{\mathbf{1\rightarrow 6\text{-}TS}}$	32.2	25.4	50.1
$\Delta E_{\mathbf{1\rightarrow 7}}$	-2.8	0.5	12.9
$\Delta H^{\neq}_{\mathbf{1\rightarrow 6\text{-}TS}}$	30.4	23.7	48.1
$\Delta H_{\mathbf{1\rightarrow 7}}$	-2.4	0.8	13.2
R=Me, L = NHC[a]			
$\Delta E^{\neq}_{\mathbf{1\rightarrow 6\text{-}TS}}$	28.2	31.8	50.3
$\Delta E_{\mathbf{1\rightarrow 7}}$	28.0	11.0	22.9
$\Delta H^{\neq}_{\mathbf{1\rightarrow 6\text{-}TS}}$	26.9	30.4	48.3
$\Delta H_{\mathbf{1\rightarrow 7}}$	28.7	11.7	23.4
R=Ph, L = NHC[a]			
$\Delta E^{\neq}_{\mathbf{1\rightarrow 6\text{-}TS}}$	28.5	30.8	49.6
$\Delta E_{\mathbf{1\rightarrow 7}}$	13.6	14.0	31.5
$\Delta H^{\neq}_{\mathbf{1\rightarrow 6\text{-}TS}}$	26.9	29.9	47.8
$\Delta H_{\mathbf{1\rightarrow 7}}$	13.7	14.8	31.5
R=Vinyl, L = NHC[a]			
$\Delta E^{\neq}_{\mathbf{1\rightarrow 6\text{-}TS}}$	26.0	24.5	45.1
$\Delta E_{\mathbf{1\rightarrow 7}}$	-14.6	-12.5	0.4
$\Delta H^{\neq}_{\mathbf{1\rightarrow 6\text{-}TS}}$	24.6	23.6	43.4
$\Delta H_{\mathbf{1\rightarrow 7}}$	-13.8	-11.7	1.2
R=Ethynyl, L = NHC[a]			
$\Delta E^{\neq}_{\mathbf{1\rightarrow 6\text{-}TS}}$	36.9	31.8	53.8
$\Delta E_{\mathbf{1\rightarrow 7}}$	-1.9	1.1	10.5
$\Delta H^{\neq}_{\mathbf{1\rightarrow 6\text{-}TS}}$	35.0	30.1	51.6
$\Delta H_{\mathbf{1\rightarrow 7}}$	-1.5	1.4	10.8

[a] NHC = 1,3-dimethylimidazol-2-ylidene

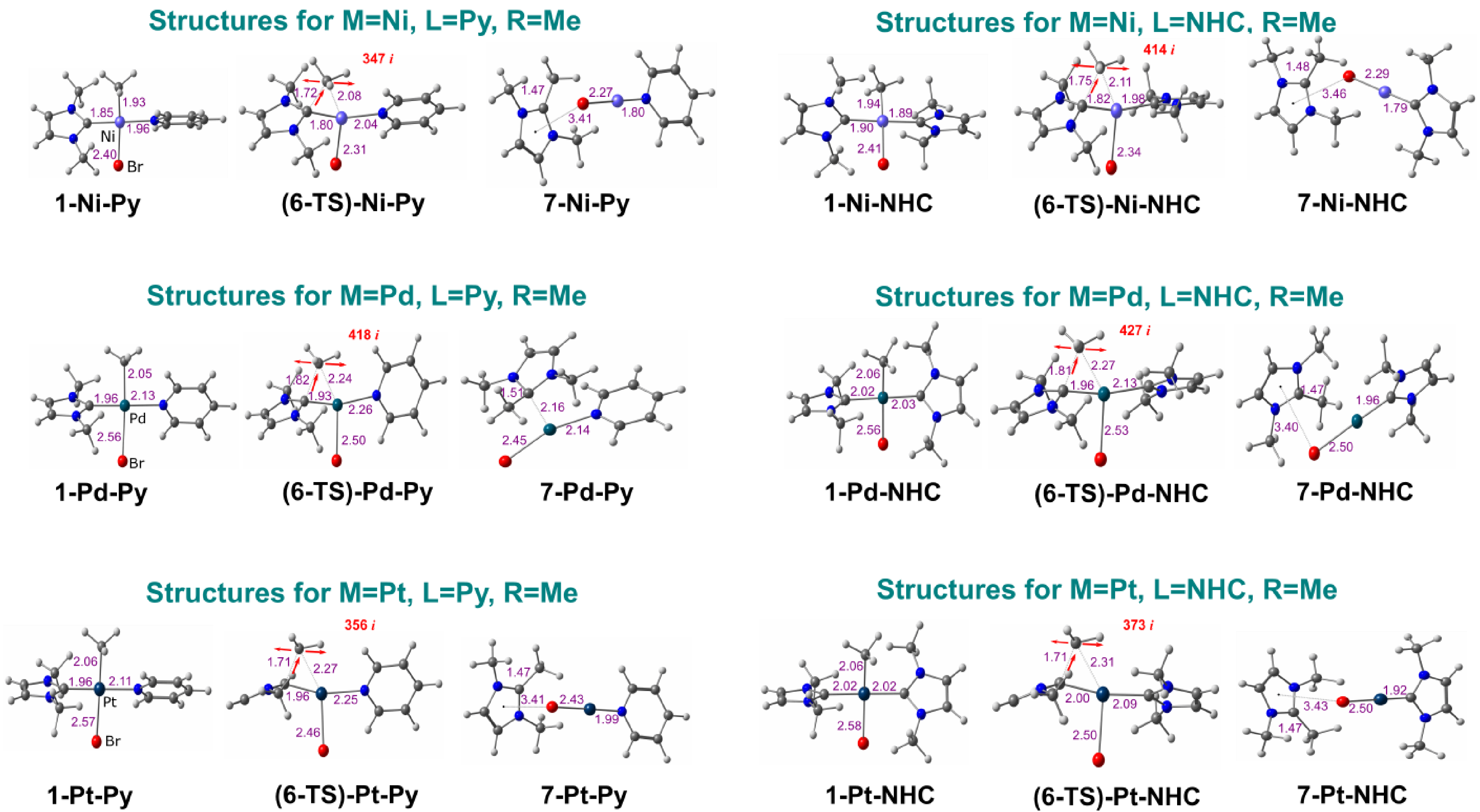

Figure S6. Optimized molecular structures of complexes **1, 7** and transition states **(6-TS)** in the Me−NHC coupling reaction. Selected bond distances (Å) are shown in purple. The atomic movements corresponding to the imaginary frequencies are depicted by red arrows.

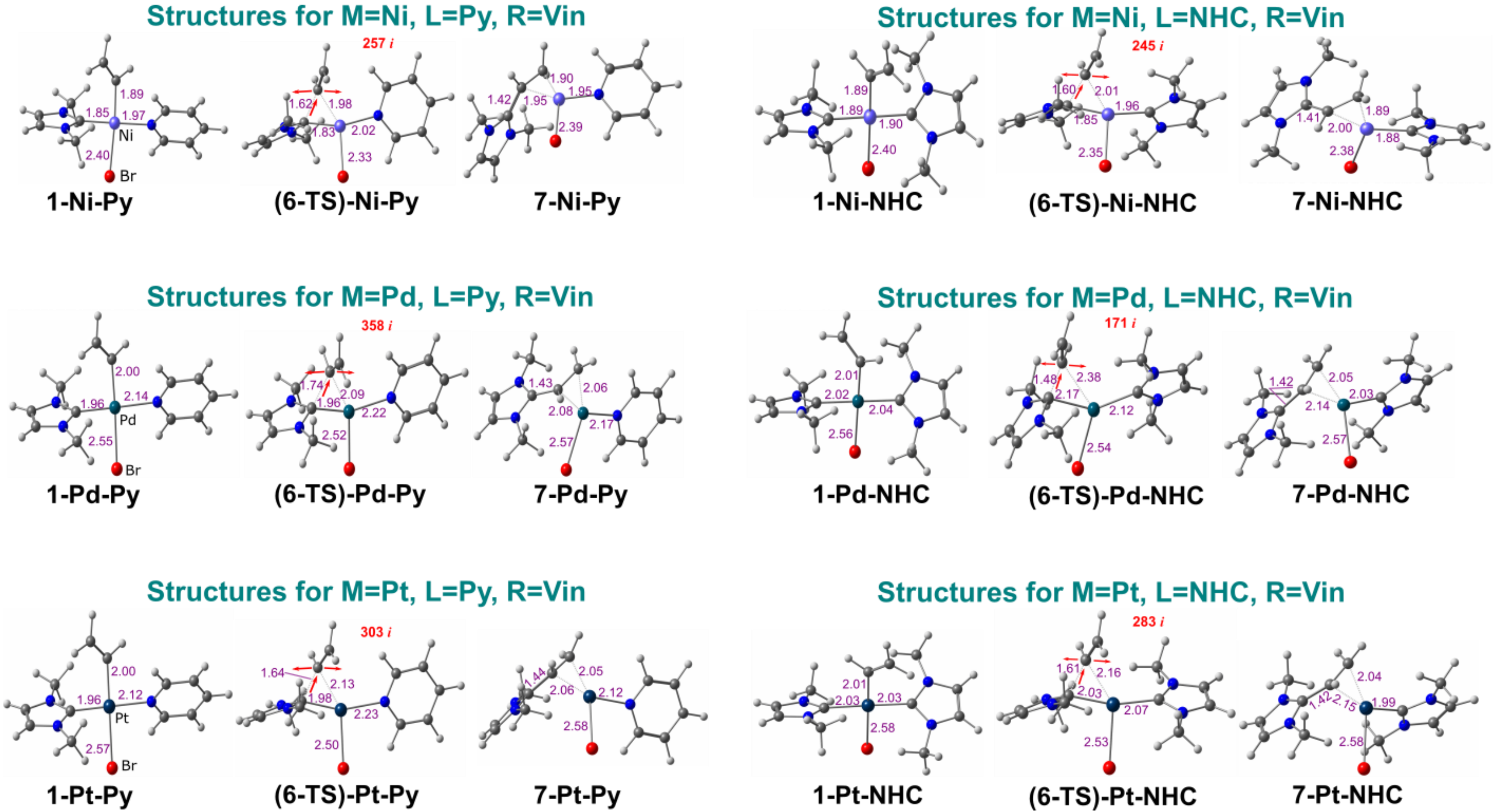

Figure S7. Optimized molecular structures of complexes **1, 7** and transition states **(6-TS)** in the Vin−NHC coupling reaction. Selected bond distances (Å) are shown in purple. The atomic movements corresponding to the imaginary frequencies are depicted by red arrows.

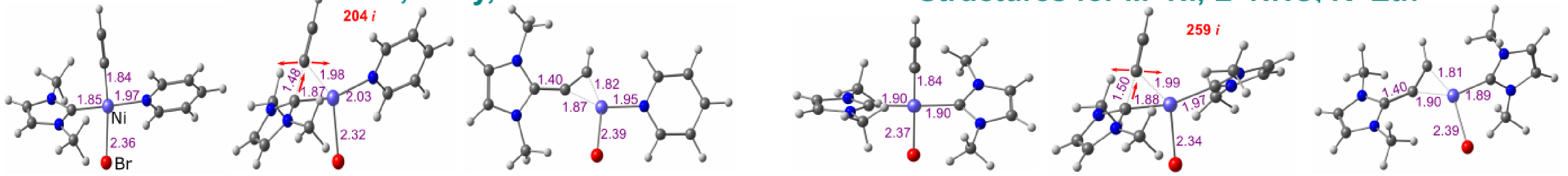

Structures for M=Ni, L=Py, R=Eth

Structures for M=Ni, L=NHC, R=Eth

1-Ni-Py **(6-TS)-Ni-Py** **7-Ni-Py** **1-Ni-NHC** **(6-TS)-Ni-NHC** **7-Ni-NHC**

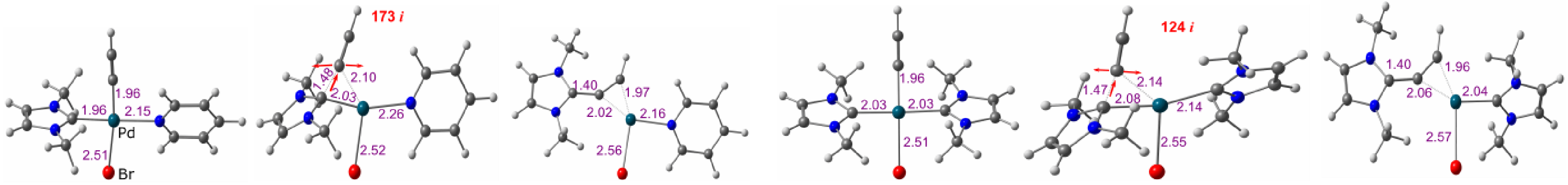

Structures for M=Pd, L=Py, R=Eth

Structures for M=Pd, L=NHC, R=Eth

1-Pd-Py **(6-TS)-Pd-Py** **7-Pd-Py** **1-Pd-NHC** **(6-TS)-Pd-NHC** **7-Pd-NHC**

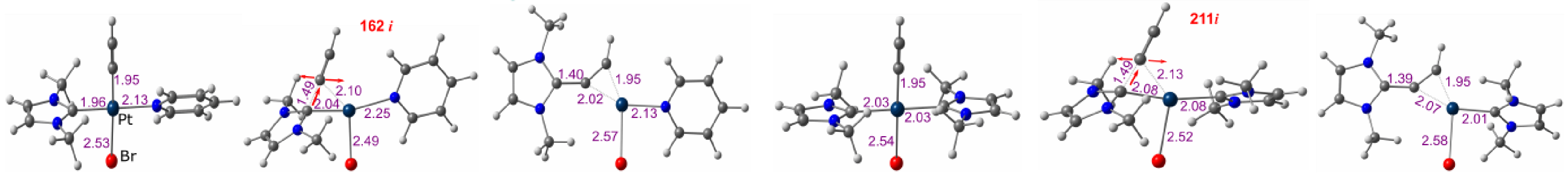

Structures for M=Pt, L=Py, R=Eth

Structures for M=Pt, L=NHC, R=Eth

1-Pt-Py **(6-TS)-Pt-Py** **7-Pt-Py** **1-Pt-NHC** **(6-TS)-Pt-NHC** **7-Pt-NHC**

Figure S8. Optimized molecular structures of complexes **1, 7** and transition states **(6-TS)** in the Eth−NHC coupling reaction. Selected bond distances (Å) are shown in purple. The atomic movements corresponding to the imaginary frequencies are depicted by red arrows.

Table S2. Activation total energies ($\Delta E^{\neq}$), activation enthalpies ($\Delta H^{\neq}$), reaction energies (ΔE) and reaction enthalpies (ΔH) for the R−NHC coupling of complexes **4** (M =Ni, Pd, Pt) at 298 K[a]

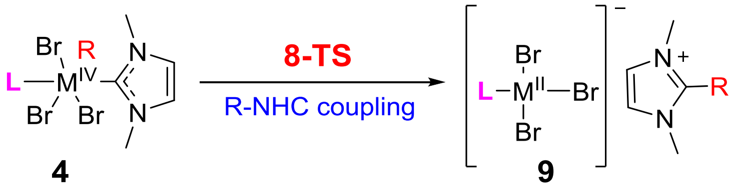

rel. energy, kcal·mol^{-1}	M = Ni	M = Pd	M = Pt
R=Me, L = Py			
$\Delta E^{\neq}_{4\rightarrow 8\text{-TS}}$	16.8	35.3	49.1
$\Delta E_{4\rightarrow 9}$	-60.9	-43.0	-17.4
$\Delta H^{\neq}_{4\rightarrow 8\text{-TS}}$	15.7	34.2	47.2
$\Delta H_{4\rightarrow 9}$	-60.0	-42.1	-16.8
R=Ph, L = Py			
$\Delta E^{\neq}_{4\rightarrow 8\text{-TS}}$	12.7	25.6	45.6
$\Delta E_{4\rightarrow 9}$	-65.4	-44.9	-17.3
$\Delta H^{\neq}_{4\rightarrow 8\text{-TS}}$	11.6	24.4	44.1
$\Delta H_{4\rightarrow 9}$	-64.5	-44.0	-16.7
R=Vinyl, L = Py			
$\Delta E^{\neq}_{4\rightarrow 8\text{-TS}}$	7.0	19.3	36.8
$\Delta E_{4\rightarrow 9}$	-62.7	-44.5	-17.6
$\Delta H^{\neq}_{4\rightarrow 8\text{-TS}}$	6.4	18.2	35.3
$\Delta H_{4\rightarrow 9}$	-61.5	-43.5	-16.8
R=Ethynyl, L = Py			
$\Delta E^{\neq}_{4\rightarrow 8\text{-TS}}$	7.2	18.9	37.6
$\Delta E_{4\rightarrow 9}$	-56.3	-39.1	-9.6
$\Delta H^{\neq}_{4\rightarrow 8\text{-TS}}$	6.2	17.6	35.7
$\Delta H_{4\rightarrow 9}$	-55.6	-38.5	-9.2
R=Me, L = NHC[a]			
$\Delta E^{\neq}_{4\rightarrow 8\text{-TS}}$	3.4	19.3	40.1
$\Delta E_{4\rightarrow 9}$	-76.0	-58.0	-35.2
$\Delta H^{\neq}_{4\rightarrow 8\text{-TS}}$	2.4	18.1	38.4
$\Delta H_{4\rightarrow 9}$	-75.2	-57.2	-34.9
R=Ph, L = NHC[a]			
$\Delta E^{\neq}_{4\rightarrow 8\text{-TS}}$	5.7	20.2	40.3
$\Delta E_{4\rightarrow 9}$	-74.3	-56.2	-31.2
$\Delta H^{\neq}_{4\rightarrow 8\text{-TS}}$	4.7	19.0	38.7
$\Delta H_{4\rightarrow 9}$	-73.5	-55.5	-30.8
R=Vinyl, L = NHC[a]			
$\Delta E^{\neq}_{4\rightarrow 8\text{-TS}}$	0.1	14.1	32.0
$\Delta E_{4\rightarrow 9}$	-72.6	-55.1	-30.5
$\Delta H^{\neq}_{4\rightarrow 8\text{-TS}}$	0.7	13.1	30.6
$\Delta H_{4\rightarrow 9}$	-71.4	-54.2	-30.0
R=Ethynyl, L = NHC[a]			
$\Delta E^{\neq}_{4\rightarrow 8\text{-TS}}$	2.3	12.7	29.5
$\Delta E_{4\rightarrow 9}$	-62.4	-49.8	-22.8
$\Delta H^{\neq}_{4\rightarrow 8\text{-TS}}$	1.4	11.5	27.9
$\Delta H_{4\rightarrow 9}$	-61.8	-49.3	-22.6

[a] NHC = 1,3-dimethylimidazol-2-ylidene

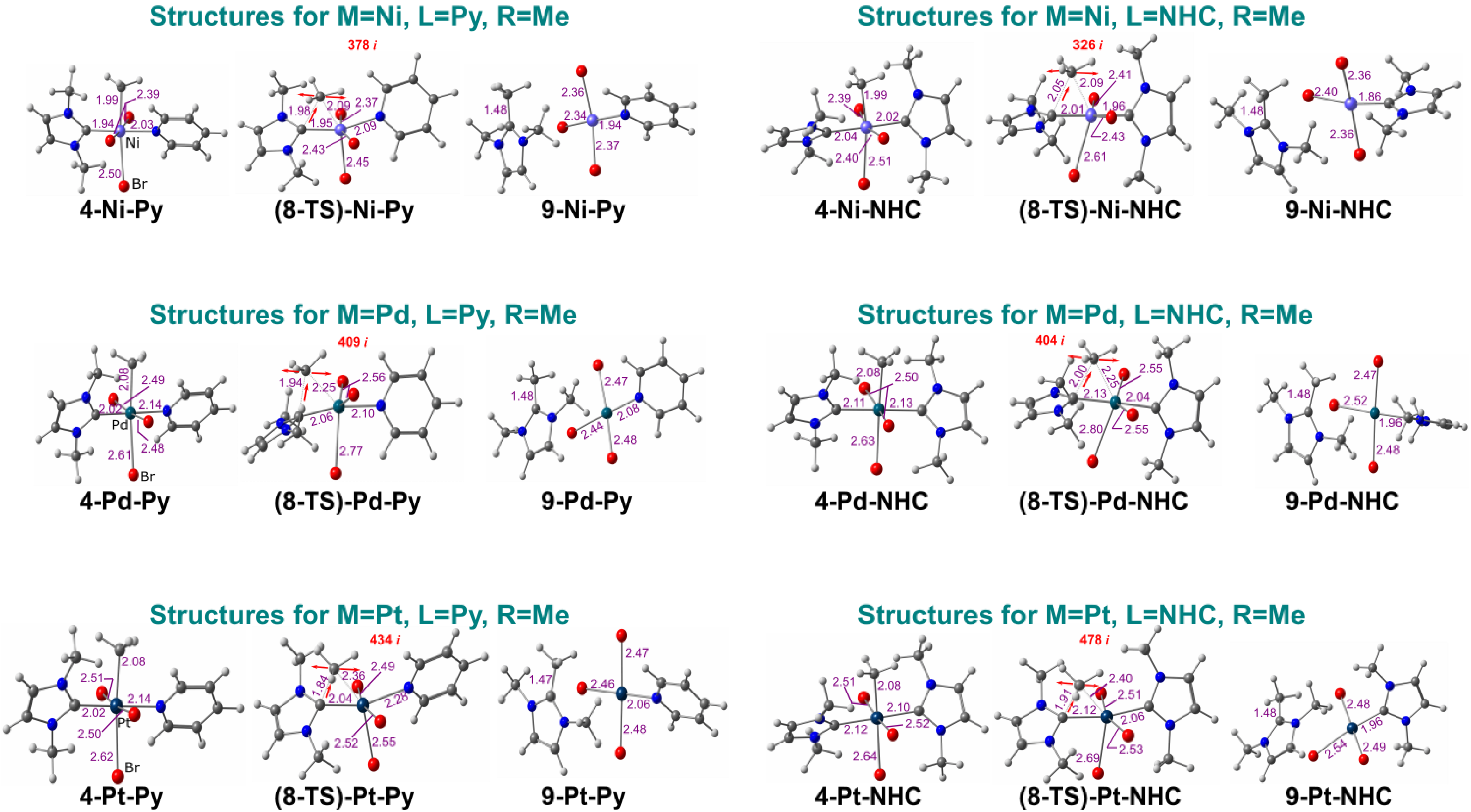

Figure S9. Optimized molecular structures of complexes **4, 9** and transition states **(8-TS)** in the Me−NHC coupling reaction. Selected bond distances (Å) are shown in purple. The atomic movements corresponding to the imaginary frequencies are depicted by red arrows.

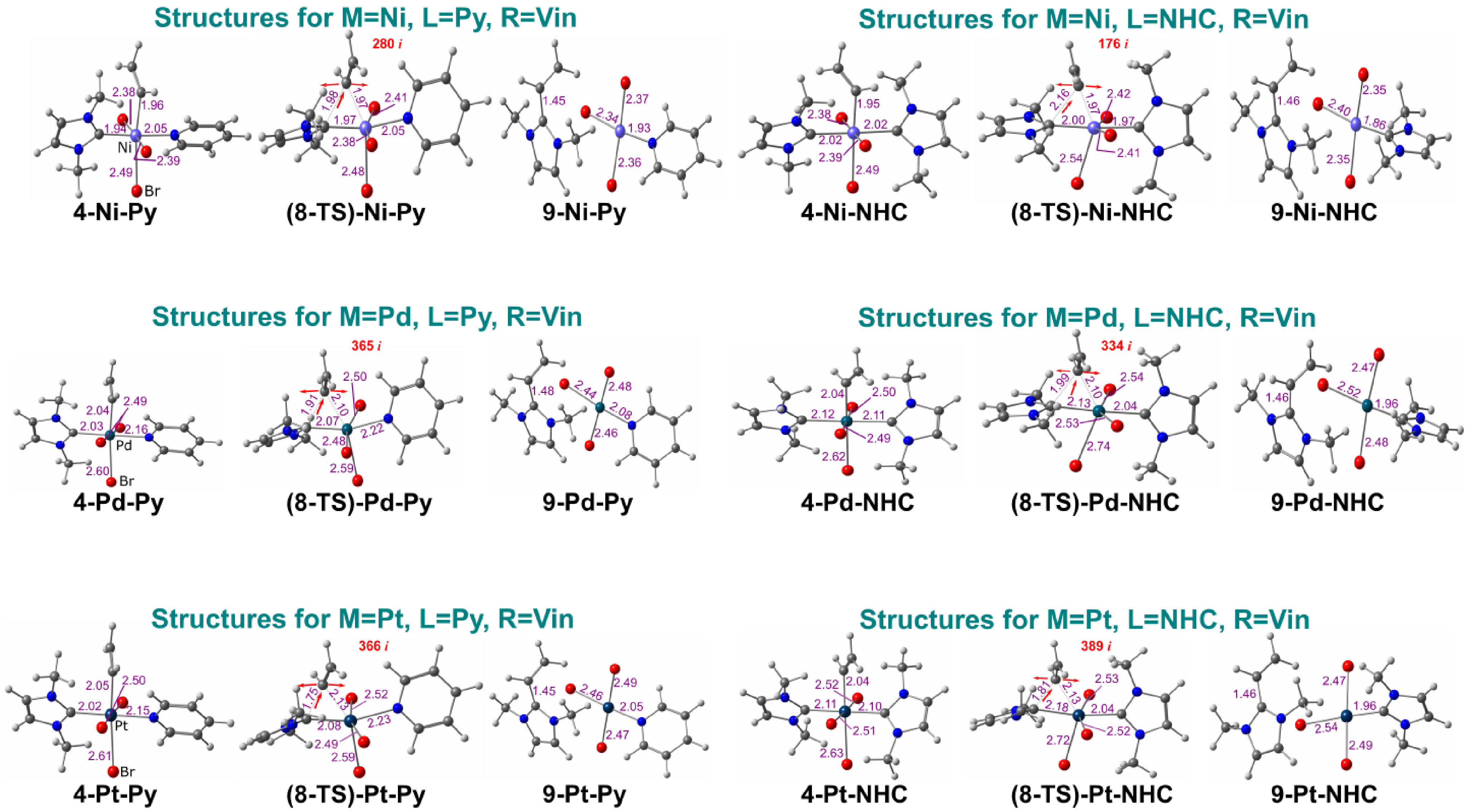

Structures for M=Ni, L=Py, R=Vin

Structures for M=Ni, L=NHC, R=Vin

Structures for M=Pd, L=Py, R=Vin

Structures for M=Pd, L=NHC, R=Vin

Structures for M=Pt, L=Py, R=Vin

Structures for M=Pt, L=NHC, R=Vin

Figure S10. Optimized molecular structures of complexes **4, 9** and transition states (**8-TS)** in the Vin−NHC coupling reaction. Selected bond distances (Å) are shown in purple. The atomic movements corresponding to the imaginary frequencies are depicted by red arrows.

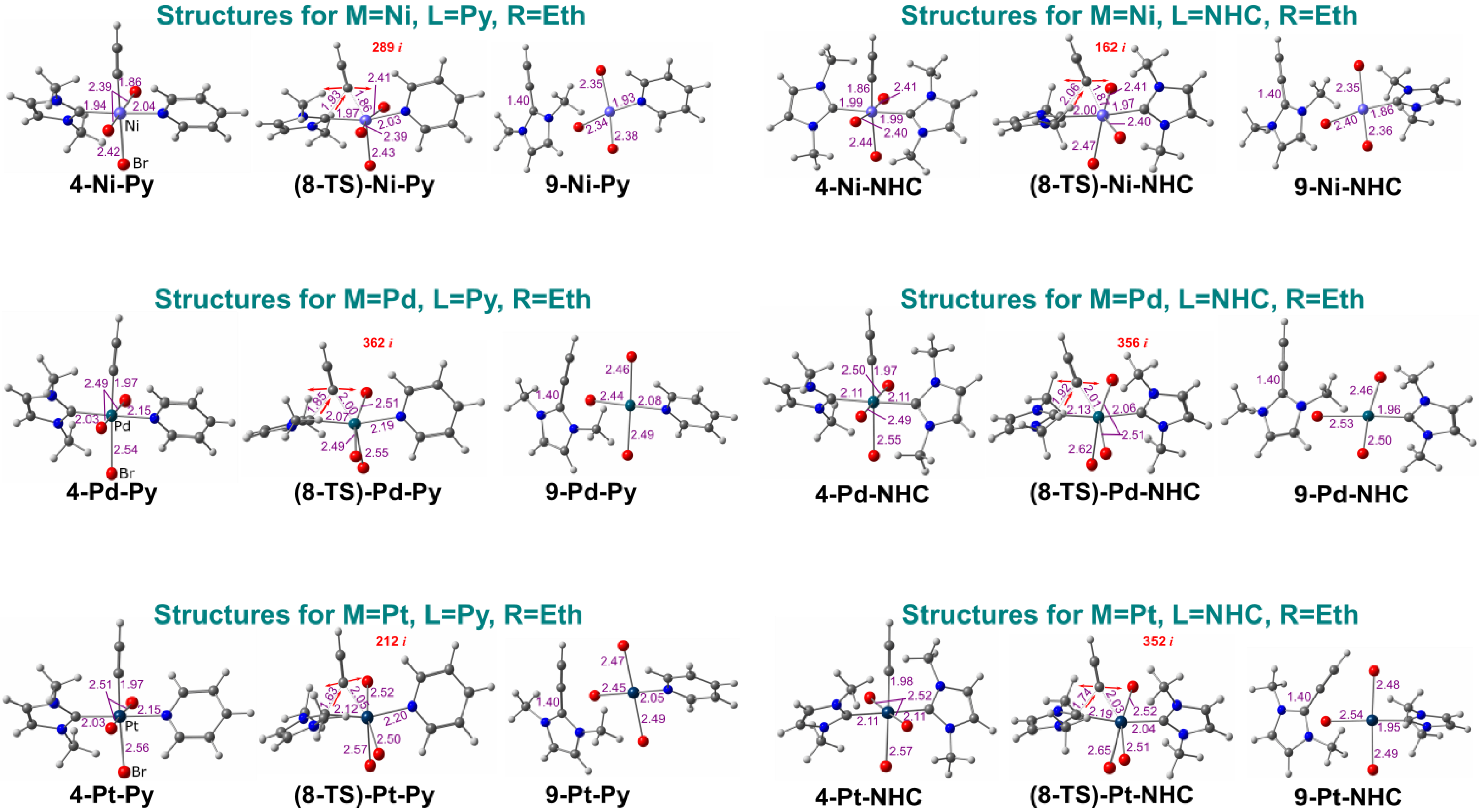

Figure S11. Optimized molecular structures of complexes **4, 9** and transition states **(8-TS)** in the Eth−NHC coupling reaction. Selected bond distances (Å) are shown in purple. The atomic movements corresponding to the imaginary frequencies are depicted by red arrows.

Table S3. Influence of NHC ligands on the activation total energies ($\Delta E^{\neq}$), activation enthalpies ($\Delta H^{\neq}$), Gibbs free energies of activation ($\Delta G^{\neq}$, kcal/mol) and reaction energies (ΔE) and reaction enthalpies (ΔH), reaction Gibbs free energies (ΔG, kcal/mol) for the Ph−NHC coupling reaction of complexes **4** (M =Ni, Pd, Pt) at 298 K.

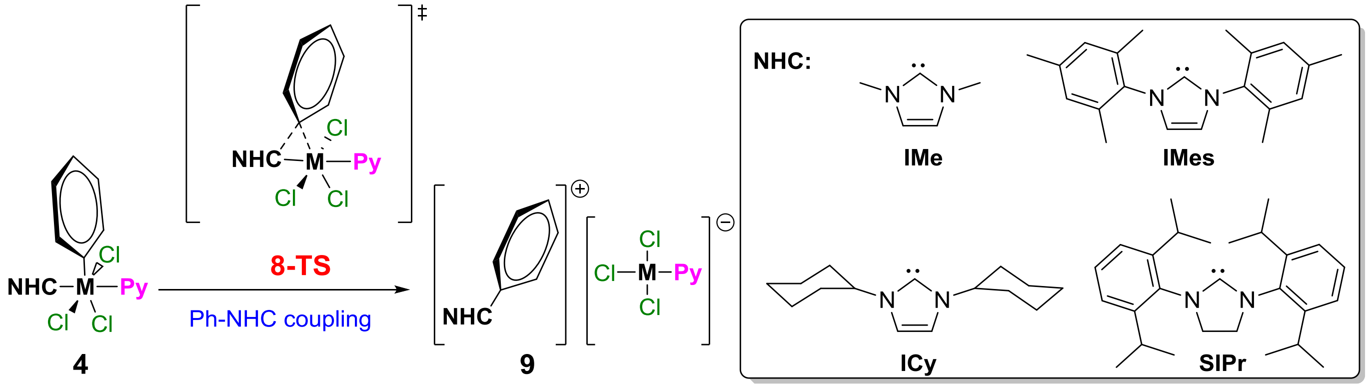

rel. energy, kcal·mol^{-1}	M = Ni	M = Pd	M = Pt
NHC = IMe			
$\Delta E^{\neq}_{4\rightarrow 8\text{-TS}}$	13.8	28.2	48.3
$\Delta E_{4\rightarrow 9}$	-60.6	-40.7	-11.8
$\Delta H^{\neq}_{4\rightarrow 8\text{-TS}}$	12.8	26.8	46.8
$\Delta H_{4\rightarrow 9}$	-59.8	-39.9	-11.1
$\Delta G^{\neq}_{4\rightarrow 8\text{-TS}}$	12.9	26.7	46.8
$\Delta G_{4\rightarrow 9}$	-65.7	-44.5	-11.8
NHC = IMes			
$\Delta E^{\neq}_{4\rightarrow 8\text{-TS}}$	9.1	22.2	42.3
$\Delta E_{4\rightarrow 9}$	-69.8	-49.3	-20.7
$\Delta H^{\neq}_{4\rightarrow 8\text{-TS}}$	7.3	20.8	40.6
$\Delta H_{4\rightarrow 9}$	-68.7	-48.9	-20.5
$\Delta G^{\neq}_{4\rightarrow 8\text{-TS}}$	8.4	21.7	41.0
$\Delta G_{4\rightarrow 9}$	-74.9	-51.7	-23.5
NHC = SIPr			
$\Delta E^{\neq}_{4\rightarrow 8\text{-TS}}$	11.1	23.5	41.2
$\Delta E_{4\rightarrow 9}$	-83.5	-62.9	-24.2
$\Delta H^{\neq}_{4\rightarrow 8\text{-TS}}$	10.4	22.5	39.8
$\Delta H_{4\rightarrow 9}$	-81.9	-61.5	-23.4
$\Delta G^{\neq}_{4\rightarrow 8\text{-TS}}$	10.8	23.8	41.2
$\Delta G_{4\rightarrow 9}$	-86.8	-66.4	-29.0
NHC = ICy			
$\Delta E^{\neq}_{4\rightarrow 8\text{-TS}}$	—	30.0	—
$\Delta E_{4\rightarrow 9}$	—	-74.5	—
$\Delta H^{\neq}_{4\rightarrow 8\text{-TS}}$	—	28.6	—
$\Delta H_{4\rightarrow 9}$	—	-73.8	—
$\Delta G^{\neq}_{4\rightarrow 8\text{-TS}}$	—	27.8	—
$\Delta G_{4\rightarrow 9}$	—	-78.6	—

Structures for NHC=IMes, M=Ni, X=Cl

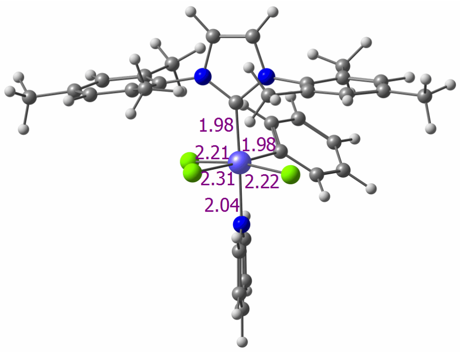

4-Ni-IMes

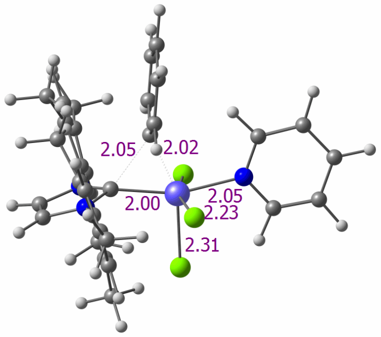

8-TS-Ni-IMes

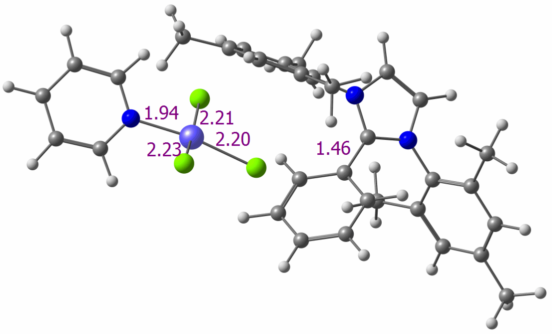

9-Ni-IMes

Structures for NHC=IMes, M=Pd, X=Cl

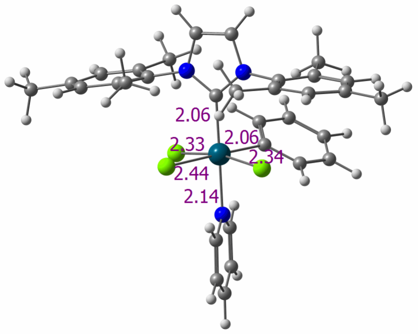

4-Pd-IMes

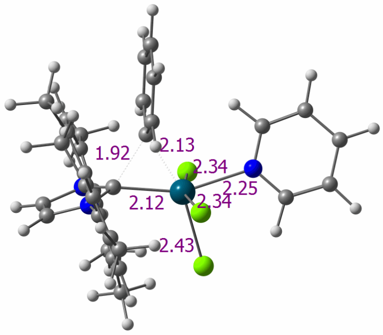

8-TS-Pd-IMes

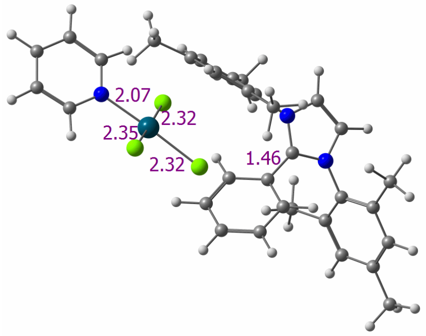

9-Pd-IMes

Structures for NHC=IMes, M=Pt, X=Cl

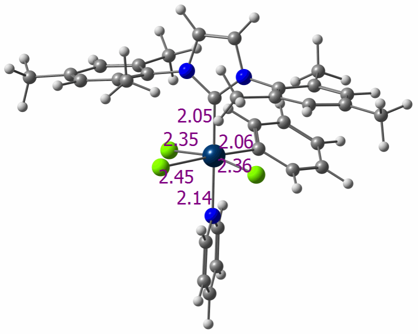

4-Pt-IMes

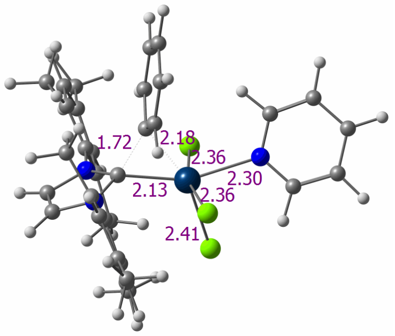

8-TS-Pt-IMes

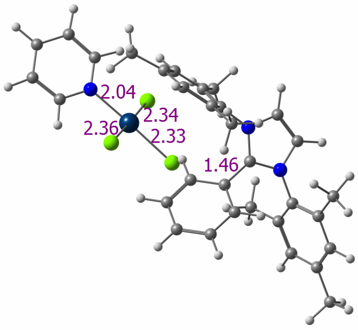

9-Pt-IMes

Figure S12. Optimized molecular structures of complexes **4, 9** and transition states **(8-TS)** in the Ph−NHC coupling reaction (NHC=IMes). Selected bond distances (Å) are shown in purple.

Structures for NHC=SIPr, M=Ni, X=Cl

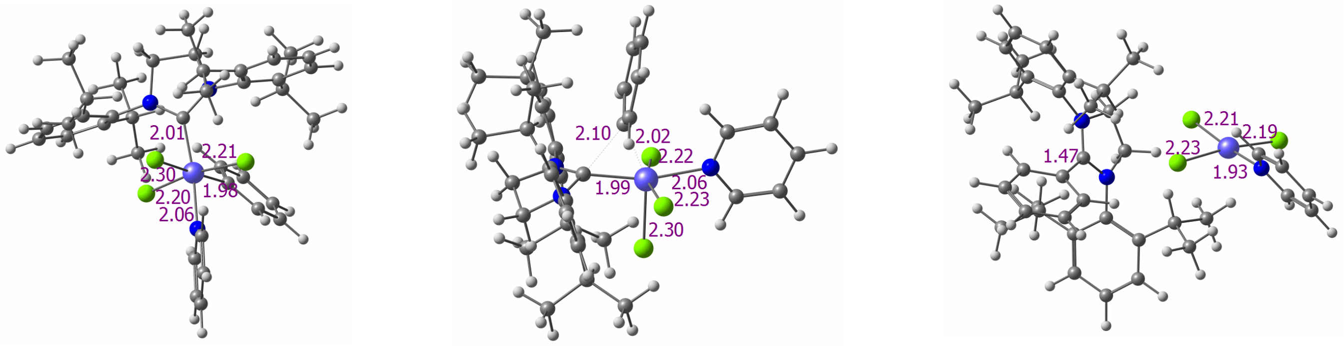

4-Ni-SIPr **8-TS-Ni-SIPr** **9-Ni-SIPr**

Structures for NHC=SIPr, M=Pd, X=Cl

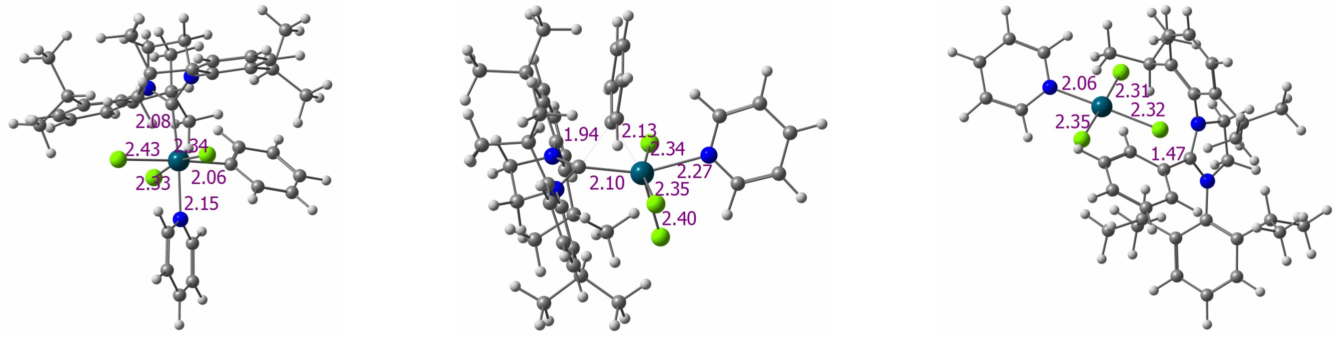

4-Pd-SIPr **8-TS-Pd-SIPr** **9-Pd-SIPr**

Structures for NHC=SIPr, M=Pt, X=Cl

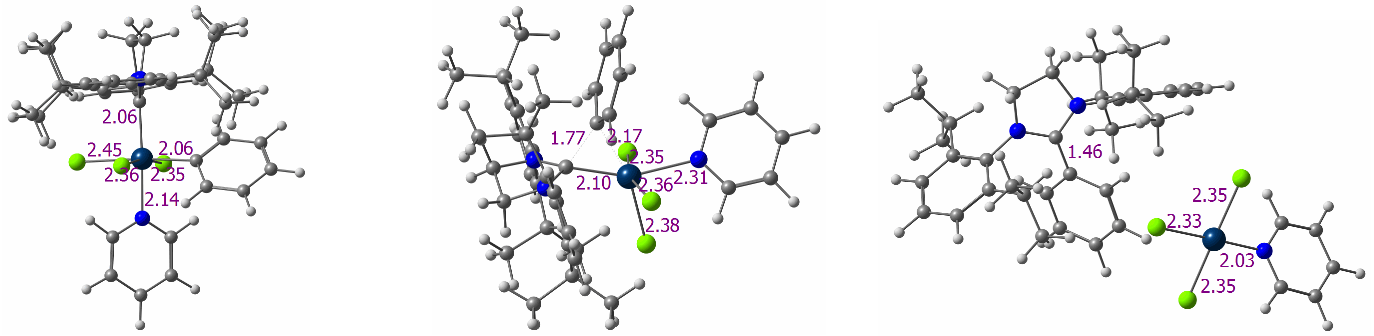

4-Pt-SIPr **8-TS-Pt-SIPr** **9-Pt-SIPr**

Figure S13. Optimized molecular structures of complexes **4, 9** and transition states **(8-TS)** in the Ph−NHC coupling reaction (NHC=SIPr). Selected bond distances (Å) are shown in purple.

Structures for NHC=ICy, M=Pd, X=Cl

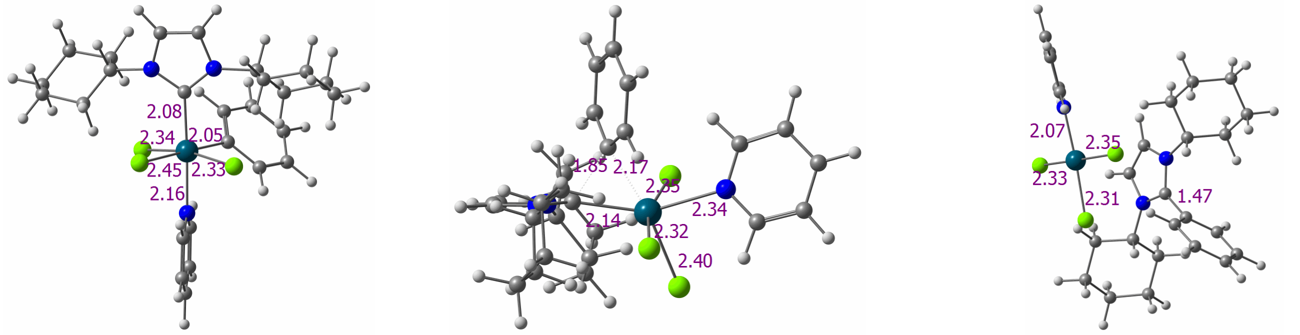

4-Pd-ICy **8-TS-Pd-ICy** **9-Pd-ICy**

Figure S14. Optimized molecular structures of complexes **4, 9** and transition states **(8-TS)** in the Ph−NHC coupling reaction (NHC=ICy). Selected bond distances (Å) are shown in purple.

Table S4. Influence of halogen ligands X (X = Cl, I) on the activation total energies ($\Delta E^{\neq}$), activation enthalpies ($\Delta H^{\neq}$), reaction energies (ΔE) and reaction enthalpies (ΔH) for the Ph–NHC coupling reaction of complexes **4** (M =Ni, Pd, Pt) at 298 K[a]

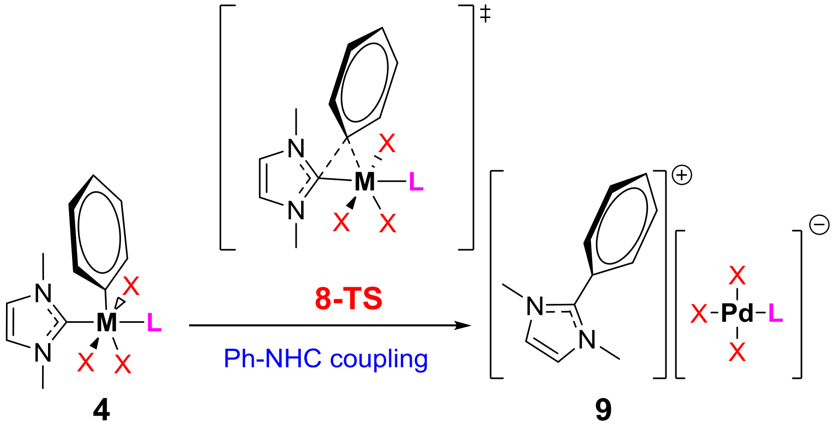

rel. energy, kcal·mol^{-1}	M = Ni	M = Pd	M = Pt
X = Cl, L = Py			
$\Delta E^{\neq}_{4\to 8\text{-TS}}$	13.8	28.2	48.3
$\Delta E_{4\to 9}$	-60.6	-40.7	-11.8
$\Delta H^{\neq}_{4\to 8\text{-TS}}$	12.8	26.8	46.8
$\Delta H_{4\to 9}$	-59.8	-39.9	-11.1
X = I, L = Py			
$\Delta E^{\neq}_{4\to 8\text{-TS}}$	11.3	22.2	42.1
$\Delta E_{4\to 9}$	-63.2	-45.9	-18.3
$\Delta H^{\neq}_{4\to 8\text{-TS}}$	10.3	20.9	40.5
$\Delta H_{4\to 9}$	-62.2	-45.1	-17.5
X = Cl, L = NHC[a]			
$\Delta E^{\neq}_{4\to 8\text{-TS}}$	9.2	24.5	44.6
$\Delta E_{4\to 9}$	-68.2	-49.6	-23.7
$\Delta H^{\neq}_{4\to 8\text{-TS}}$	8.3	23.4	43.1
$\Delta H_{4\to 9}$	-67.6	-49.0	-23.3
X = I, L = NHC[a]			
$\Delta E^{\neq}_{4\to 8\text{-TS}}$	1.8	14.2	33.3
$\Delta E_{4\to 9}$	-78.0	-62.0	-36.7
$\Delta H^{\neq}_{4\to 8\text{-TS}}$	0.7	13.1	32.2
$\Delta H_{4\to 9}$	-77.3	-61.3	-36.1

[a] NHC = 1,3-dimethylimidazol-2-ylidene

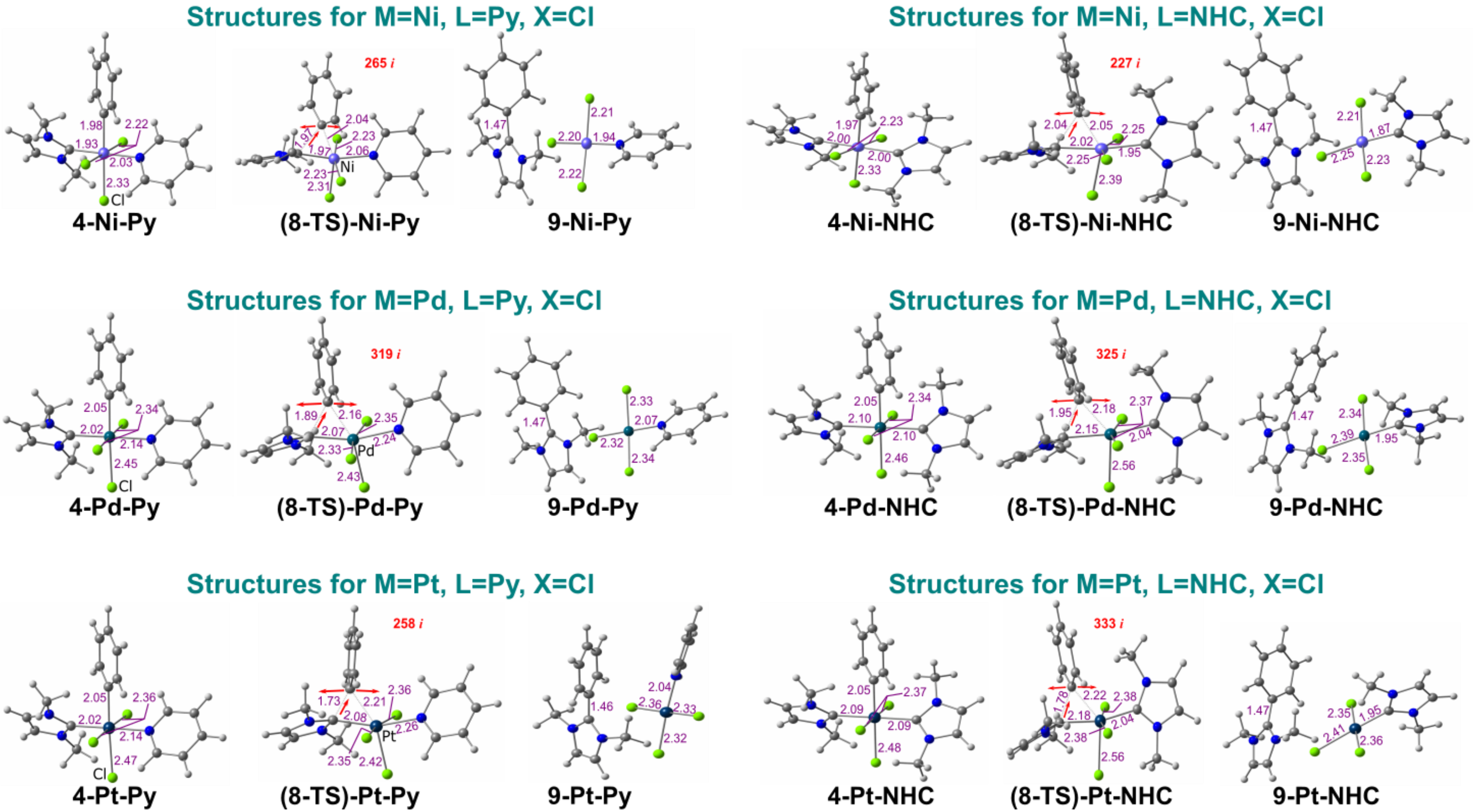

Figure S15. Optimized molecular structures of complexes **4, 9** and transition states **(8-TS)** in the Ph−NHC coupling reaction. Selected bond distances (Å) are shown in purple. The atomic movements corresponding to the imaginary frequencies are depicted by red arrows.

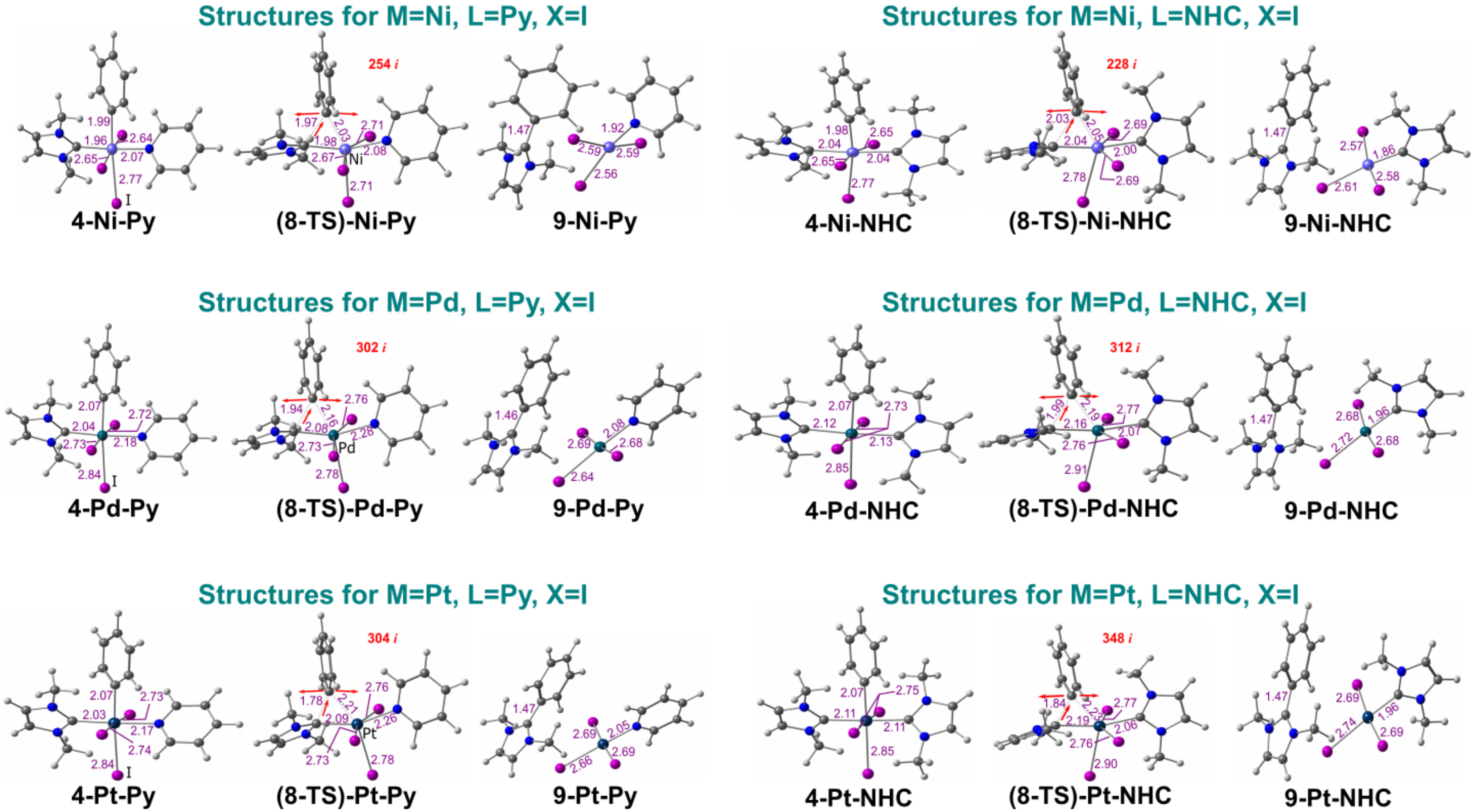

Figure S16. Optimized molecular structures of complexes **4, 9** and transition states **(8-TS)** in the Ph−NHC coupling reaction. Selected bond distances (Å) are shown in purple. The atomic movements corresponding to the imaginary frequencies are depicted by red arrows.

Table S5. Reaction energies (ΔE), reaction enthalpies (ΔH) and reaction Gibbs free energies (ΔG) for the Br−NHC coupling of complexes **1** (M =Ni, Pd, Pt) at 298 K[a]

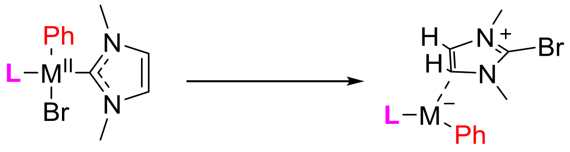

1 **13**

rel. energy, kcal·mol^{-1}	M = Ni	M = Pd	M = Pt
L = Py			
$\Delta E_{1\rightarrow13}$	98.3	89.0	94.1
$\Delta H_{1\rightarrow13}$	96.5	87.3	92.6
$\Delta G_{1\rightarrow13}$	95.9	86.8	92.2
L = NHC[a]			
$\Delta E_{1\rightarrow13}$	100.2	90.5	95.0
$\Delta H_{1\rightarrow13}$	98.1	89.2	93.4
$\Delta G_{1\rightarrow13}$	97.6	87.4	93.5

[a] NHC = 1,3-dimethylimidazol-2-ylidene

Structures for L=Py

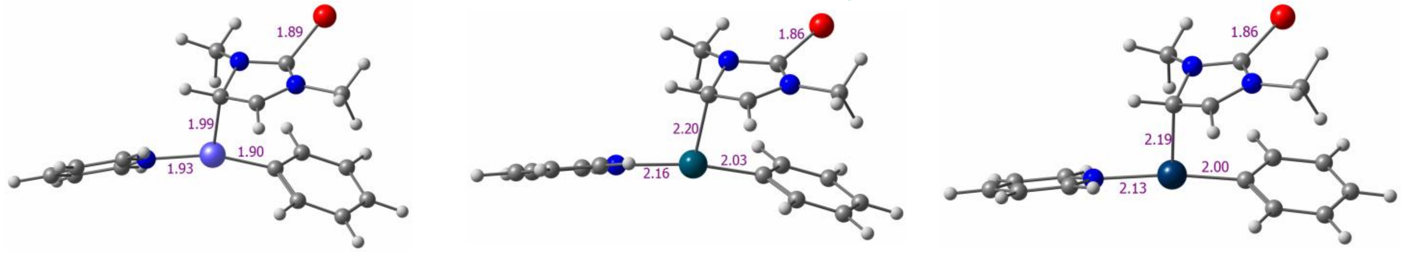

13-Ni-Py **13-Pd-Py** **13-Pt-Py**

Structures for L=NHC

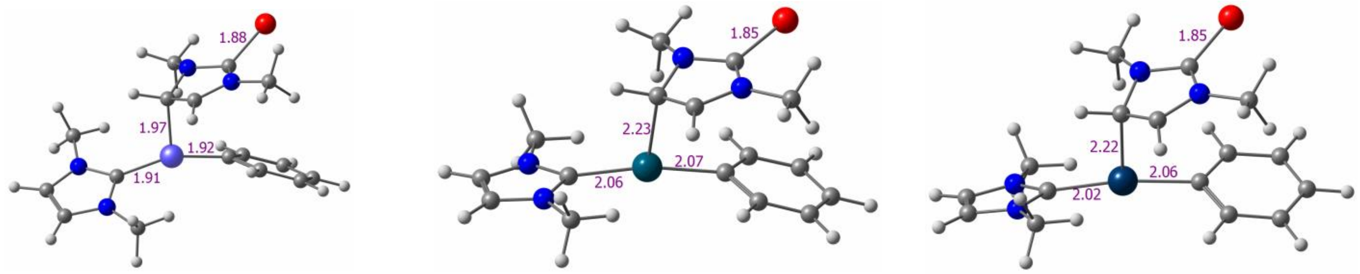

13-Ni-NHC **13-Pd-NHC** **13-Pt-NHC**

Figure S17. Optimized molecular structures of complexes **13** calculated at the PBE1PBE/6-311+G(d)&SDD

Table S6. Activation total energies ($\Delta E^{\neq}$), activation enthalpies ($\Delta H^{\neq}$), reaction energies (ΔE) and reaction enthalpies (ΔH) for the Br–NHC coupling of complexes **4** (M =Ni, Pd, Pt) at 298 K[a]

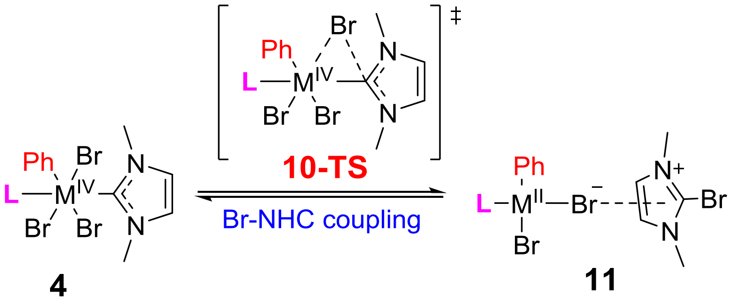

rel. energy, kcal·mol^{-1}	M = Ni	M = Pd	M = Pt
L = Py			
$\Delta E^{\neq}_{\mathbf{4\rightarrow10\text{-}TS}}$	19.8	28.9	44.1
$\Delta E_{\mathbf{4\rightarrow11}}$	-8.9	4.9	28.0
$\Delta H^{\neq}_{\mathbf{4\rightarrow10\text{-}TS}}$	17.9	27.1	42.9
$\Delta H_{\mathbf{4\rightarrow11}}$	-9.5	4.4	27.4
L = NHC[a]			
$\Delta E^{\neq}_{\mathbf{4\rightarrow10\text{-}TS}}$	17.3	30.7	47.8
$\Delta E_{\mathbf{4\rightarrow11}}$	-15.2	-1.9	17.6
$\Delta H^{\neq}_{\mathbf{4\rightarrow10\text{-}TS}}$	15.5	28.8	45.9
$\Delta H_{\mathbf{4\rightarrow11}}$	-16.1	-2.8	16.6

[a] NHC = 1,3-dimethylimidazol-2-ylidene

Structures for L=Py

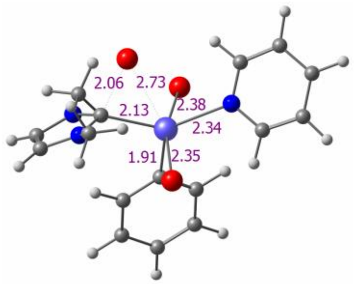

(10-TS)-Ni-Py

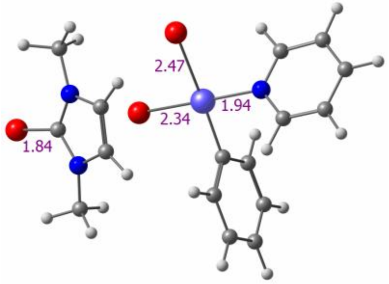

11-Ni-Py

Structures for L=NHC

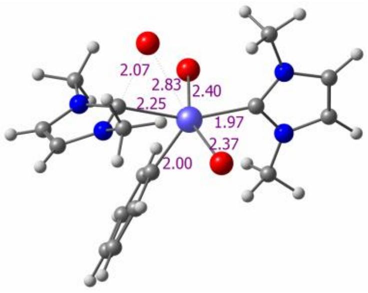

(10-TS)-Ni-NHC

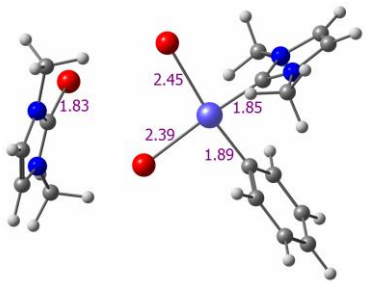

11-Ni-NHC

Structures for L=Py

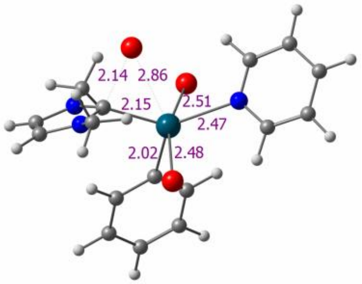

(10-TS)-Pd-Py

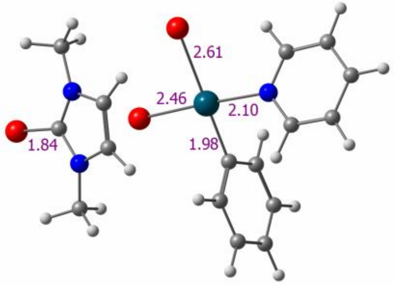

11-Pd-Py

Structures for L=NHC

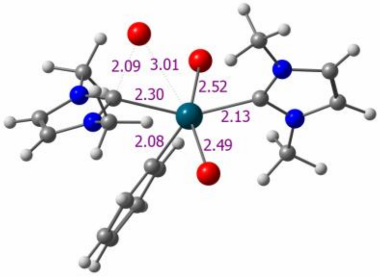

(10-TS)-Pd-NHC

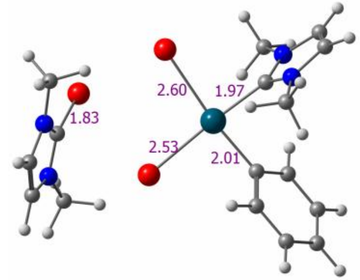

11-Pd-NHC

Structures for L=Py

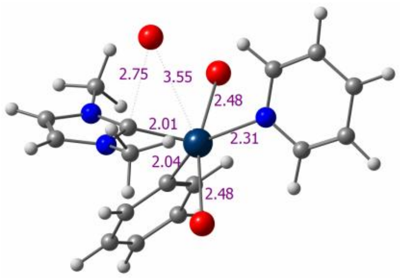

(10-TS)-Pt-Py

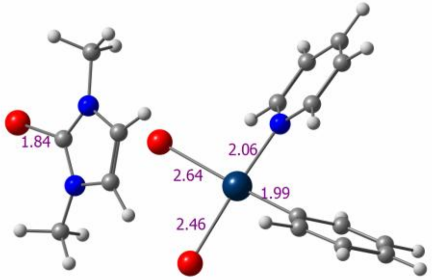

11-Pt-Py

Structures for L=NHC

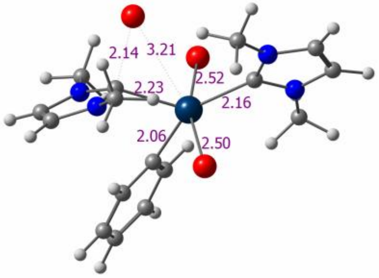

(10-TS)-Pt-NHC

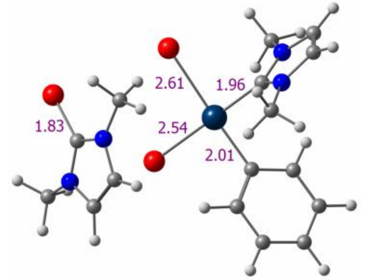

11-Pt-NHC

Figure S18. Optimized geometries of complexes **10-TS** and **11** in the Br−NHC coupling reaction calculated at the PBE1PBE/6-311+G(d)&SDD. Selected bond distances (Å) are shown in purple.

Table S7. Activation total energies ($\Delta E^{\neq}$), activation enthalpies ($\Delta H^{\neq}$), reaction energies (ΔE) and reaction enthalpies (ΔH) for the Br−Br reductive elimination from complexes **4** (M =Ni, Pd, Pt) at 298 K[a]

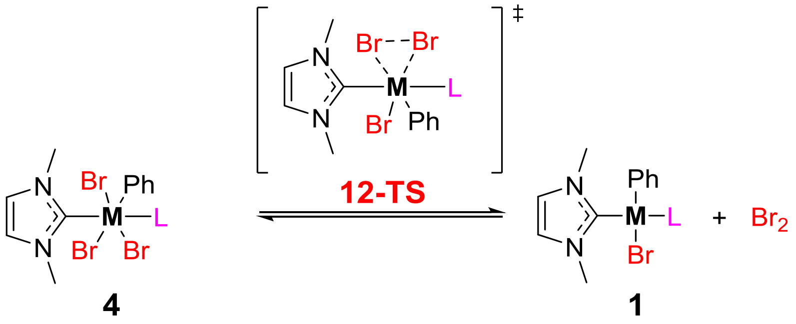

rel. energy, kcal·mol^{-1}	M = Ni	M = Pd	M = Pt
L = Py			
$\Delta E^{\neq}_{4\rightarrow 12\text{-TS}}$	28.5	34.8	58.9
$\Delta E_{4\rightarrow(1+Br2)}$	1.7	15.4	29.2
$\Delta H^{\neq}_{4\rightarrow 12\text{-TS}}$	27.5	33.9	57.8
$\Delta H_{4\rightarrow(1+Br2)}$	0.0	13.7	27.4
L = NHC[a]			
$\Delta E^{\neq}_{4\rightarrow 12\text{-TS}}$	28.4	39.9	53.7
$\Delta E_{4\rightarrow(1+Br2)}$	-2.2	11.8	23.5
$\Delta H^{\neq}_{4\rightarrow 12\text{-TS}}$	27.2	38.6	52.5
$\Delta H_{4\rightarrow(1+Br2)}$	-4.3	9.1	21.3

[a] NHC = 1,3-dimethylimidazol-2-ylidene

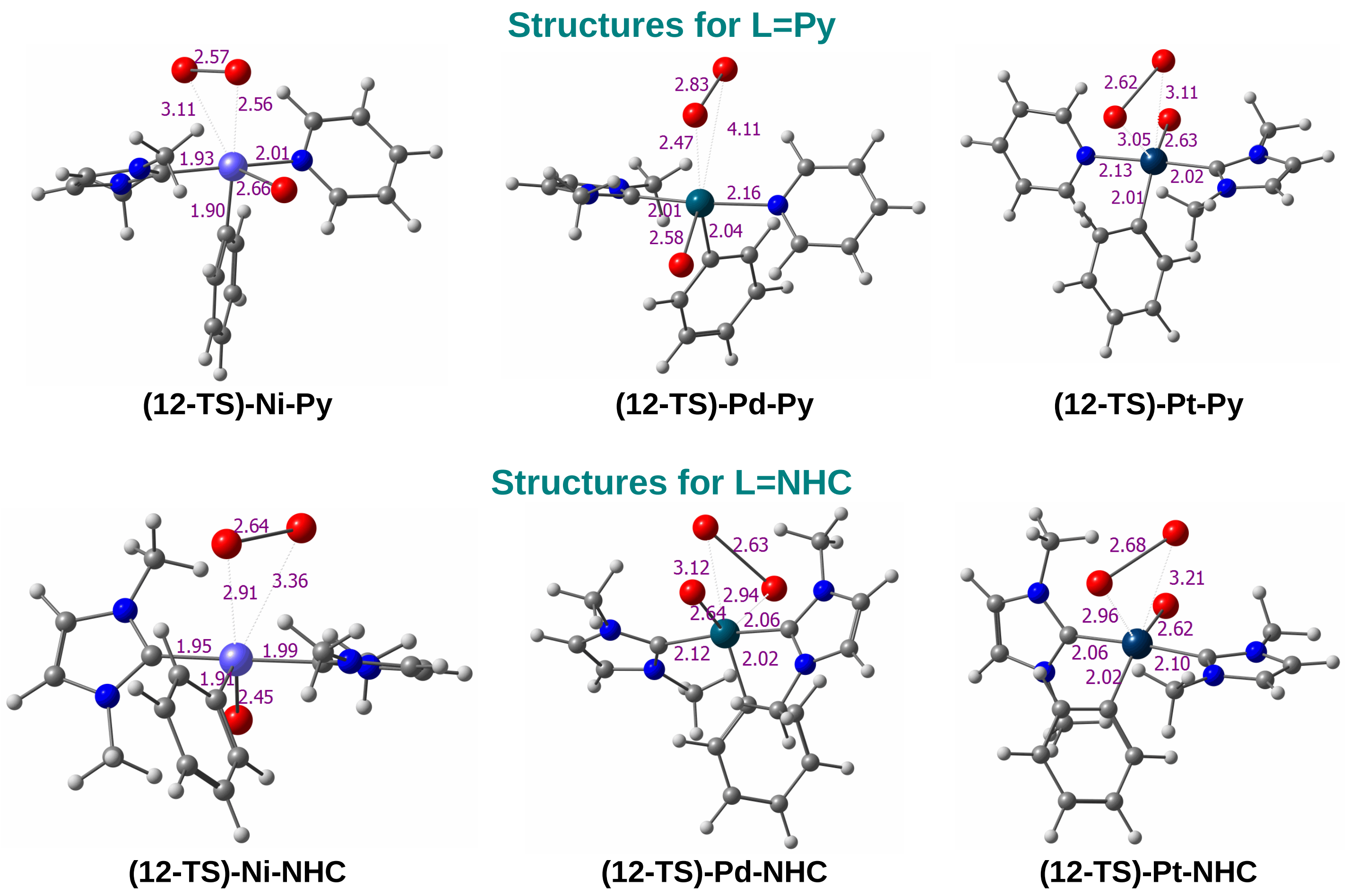
Structures for L=Py

(12-TS)-Ni-Py **(12-TS)-Pd-Py** **(12-TS)-Pt-Py**

Structures for L=NHC

(12-TS)-Ni-NHC **(12-TS)-Pd-NHC** **(12-TS)-Pt-NHC**

Figure S19. Optimized geometries of transition states **(12-TS)** calculated at the PBE1PBE/6-311+G(d)&SDD

Table S8. Equilibrium potentials E_0 for oxidation of Ni^{2+}, Pd^{2+} and Pt^{2+} ions in aqueous solutions to give corresponding metal oxides[a,b]

Reaction	E_0 (V)
$Ni^{2+}_{(aq.)} + 2H_2O = NiO_2 + 4H^+ + 2e^-$	$E_0 = 1.593 – 0.1182pH – 0.0295\log[Ni^{2+}]$
$Pd^{2+}_{(aq.)} + 2H_2O = NiO_2 + 4H^+ + 2e^-$	$E_0 = 1.194 – 0.1182pH – 0.0295\log[Pd^{2+}]$
$Pt^{2+}_{(aq.)} + 2H_2O = NiO_2 + 4H^+ + 2e^-$	$E_0 = 0.837 – 0.1182pH – 0.0295\log[Pt^{2+}]$

[a] The presented data were taken from: *Atlas of Electrochemical Equilibria in Aqueous Solutions,* ed. M. Pourbaix, National Association of Corrosion Engineers, Houston, Texas, USA, 1974, 644 p.

[b] The E_0 reflect thermodynamic proneness of cations M^{2+} to oxidation: than the E_0 value is lower than the equilibrium is significantly shifted to the right.